

Growth-Induced Evolution of Polarity in Organic Crystals

J. Hulliger,^{*,†} H. Bebie,[‡] S. Kluge,[†] and A. Quintel[†]

Department of Chemistry and Biochemistry, University of Berne, Freiestrasse 3, CH-3012 Berne, Switzerland, and Institute for Theoretical Physics, University of Berne, Sidlerstrasse 5, CH-3012 Berne, Switzerland

Received June 15, 2001. Revised Manuscript Received January 2, 2002

A Markov-mean-field model is developed to describe growth-induced polarity in single-component organic crystals formed by dipolar molecules. Results of an analytical theory agree well with corresponding Monte Carlo simulations. Polarity formation is analyzed in terms of three basic energy differences, two of them resulting from the interaction of functional groups (synthons) and a third one accounting for the lateral interaction. Basic packing types are discussed with respect to polarity formation. The Markov model provides a general description of the phenomenological behavior when moving energetically from centric to polar structures. Keeping synthon interactions within reasonable limits, the range for designing lateral coupling is limited to a few kilojoules per mole for a square lattice: Between a gap of about $-2 \text{ kJ/mol} \leq \Delta E_{\perp} \leq 3-4 \text{ kJ/mol}$ (300 K), the stochastic process of orientational disorder is either significantly increasing (centric structures) or decreasing (polar structures) polarity. Outside of these borders, orientational disorder represents only a small perturbation to centric or polar structures. With respect to the existence of structure types, the model predicts that a molecular packing where the lateral energy difference between a parallel and an antiparallel alignment of molecules is larger than about 3 kJ/mol (square lattice, 300 K) most likely results in a centric structure featuring a low level of orientational disorder. A fundamentally new behavior for the growth of polar crystals is predicted: As a consequence of the Markov model, one of the two inequivalent growth directions of a polar axis is metastable against a 180° flipping of most of the dipoles. This type of a continuous process of twinning is different from geometrical twinning. A first set of data on real crystals is given, demonstrating polarity formation in crystal structures for which the X-ray analysis has reported only centric space groups.

Introduction

The classical view on how polarity of a macroscopic organic crystal comes about is as follows:¹ A highly cooperative process called nucleation is creating a supercritical seed, which may show similarity to the later crystal structure. By further attachments of molecules, such aggregates grow to macroscopic size, essentially by a mechanism of *replication*. It is possible that during the growth of a nanocrystal structural changes occur. A number of polymorphs² may be formed including the possibility of a polar or even ferroelectric phase. It has become an attempt of materials chemistry and crystal engineering to control the process of nucleation for obtaining polymorphic forms featuring polar or other properties.³

Recently,^{4–6} we have introduced a general concept that does not focus on the importance of controlling the

formation of a polar state at the level of nucleation. A polar but macroscopically twinned state can just be the result of growth, *irrespective of the existence of polarity for a seed*. The basics of both the classical (i) and the new approach (ii) are summarized in Figure 1: Following the classical model i, crystal engineering will have to control polarity formation at the step of nucleation. By virtue of an evolutionary mechanism ii, a seed crystal may show no polarity; however, polarity can evolve during growth to macroscopic size.

Although we have shown previously^{4–6} that dipolar molecules that we consider here (see Table 1) principally fall into class ii, there are, of course, compounds that merely belong to class i, just because the level of orientational disorder which one may find experimentally is very low. Theoretical and experimental⁷ studies

* To whom correspondence should be addressed. E-mail: juerg.hulliger@iac.unibe.ch.

[†] Department of Chemistry and Biochemistry.

[‡] Institute for Theoretical Physics.

(1) Hurlle, D. T. J. *Handbook of Crystal Growth*; Elsevier Science Publishers: Amsterdam, The Netherlands, 1993; Vol. 1.

(2) Bernstein, J.; Davey, J. R.; Henck, J.-O. *Angew. Chem., Int. Ed.* **1999**, *38*, 3441.

(3) Sharma, S.; Radhakrishnan, T. P. *J. Phys. Chem. B* **2000**, *104*, 10191.

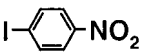
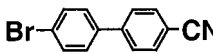
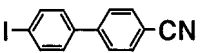
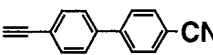
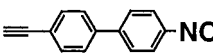


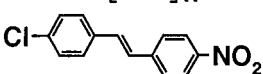
(4) Hulliger, J. Z. *Kristallogr.* **1999**, *214*, 9.

(5) (a) Hulliger, J.; Roth, S. W.; Quintel, A.; Bebie, H. *J. Solid State Chem.* **2000**, *152*, 49. (b) Hulliger, J.; Langley, P. J.; Roth, S. W. *Cryst. Eng.* **1998**, *1*, 177–189.

(6) Hulliger, J.; Roth, S. W.; Quintel, A. In *Crystal Engineering: From Molecules to Materials*; Braga, D., Grepioni, F., Orpen, A. G., Eds.; Kluwer Academic Publishers: Dordrecht, The Netherlands, 1999; pp 349–368.

(7) (a) Hulliger, J.; König, O.; Hoss, R. *Adv. Mater.* **1995**, *7*, 719. (b) Hoss, R.; König, O.; Kramer-Hoss, V.; Berger, U.; Rogin, P.; Hulliger, J. *Angew. Chem., Int. Ed. Engl.* **1996**, *35*, 1664.

Table 1. Examples of Centric Crystals Structures (According to an X-ray Determination) Showing SHG Effects

compounds and refs	crystal preparation	purity (mol %)	space group (R values)	synthons	SHG activity
1  (21)	temperature lowering, EtOH	≥ 99.9	$P\bar{1}$ ($wR_2 = 0.042$)	$-I \cdots O_2N-$	\ll urea
2  (22)	sublimation, $T = 100^\circ\text{C}$	≥ 99.9	$P2_1/c$ ($R = 0.079$)	$-Br \cdots NC-$	$<$ urea
3  (23)	temperature lowering, EtOH	≥ 99.9	$P2_1/c$ ($R = 0.043$)	$-I \cdots NC-$	$=$ urea
4  (24)	temperature lowering, EtOH	≥ 99.8	$P\bar{1}$ ($wR_2 = 0.143$)	$\equiv CH \cdots NC-$	$<$ urea
5  (24)	temperature lowering, EtOH	≥ 99.8	$P\bar{1}$ ($wR_2 = 0.151$)	$\equiv CH \cdots O_2N-$	$<$ urea
6  (25)	solvent evaporation, $\text{CH}_2\text{Cl}_2/\text{hexane}$	≥ 99.8	$Pbcn$ ($R = 0.070$)	$-NH_2 \cdots O_2N-$	0.04–0.2 times urea ^a
7  $n = 2, 3$ (25)	solvent evaporation, CH_3CN	≥ 99.8	$P2_1/c$ ($R = 0.076; 0.056$)	$-NH_2 \cdots O_2N-$	0.02; 0.03 times urea ^a
8  (26)	sublimation, $T = 165^\circ\text{C}$ and different solvents (26)	$\geq 98.0^b$	$P2_1/c$ ($wR_2 = 0.163$)	weak interactions, $C-H \cdots O_2N-$, $C-H \cdots Cl-$	2.8–11 times urea

^a In this case, authors used polycrystalline samples. Polymorphs of **6** and **7** are not reported. ^b Impurity: *z* isomer, this work.

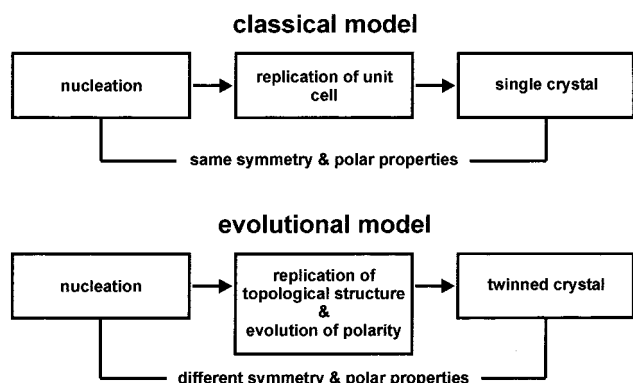


Figure 1. Comparison of the classical and evolutionary models on the origin of polarity in molecular crystals built of dipolar molecules.

have shown, however, that particular materials undoubtedly belong to class ii. Basic features of polar growth for class ii materials are accessible by scanning pyroelectric microscopy⁸ (SPEM) and phase-sensitive second harmonic microscopy⁹ (PS-SHM). For a review on these techniques, see ref 10.

For the purpose of an elementary introduction to a mechanism of growth producing a *vector-type* property such as electrical polarity, let us start from achiral but acentric building blocks. During the growth of whatever crystal structure, building blocks will be attached to faces (Figure 2) of a seed crystal (no theory on nucleation is being presented here). Because in our description we have reduced building blocks to a vector representing the dipole moment of an A,D-disubstituted spacer, we allow for only 1 degree of freedom for disorder: We have either a “down” (\downarrow) or an “up” (\uparrow) orientation of arrows, if attached to a surface (Figure 2). Attachments where dipoles are parallel to a face are not considered for further discussion here.

The system of molecules attached to a face shall be defined as such: We assume an *adlayer* of dipolar

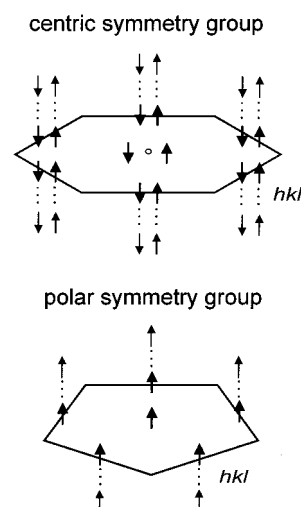


Figure 2. Illustration of two basically different situations if growth at faces (hkl) of a *centric* (upper) or a *polar* (lower) seed is occurring. The circle is indicating a center of symmetry, which is lost at the surface. Therefore, faulted attachments of \downarrow and \uparrow molecules are associated with a different energy of defect formation.

molecules attached to a surface (substrate) layer grown from the same molecules. Thermalization, i.e., establishment of the equilibrium state with respect to a \downarrow vs \uparrow orientation, is allowed only for the adlayer. Thermodynamic arguments including the effect of configurational entropy in the term for the free energy F describing the adlayer show that at temperature T the adlayer undergoes orientational disorder, irrespective of the packing type of molecules ($\downarrow\downarrow\downarrow\dots$ polar or $\downarrow\uparrow\uparrow\dots$ centric). In case intermolecular interactions favor a centric arrangement of dipoles (vector sum being strictly zero), the F energy can be lowered by introducing *faulted orientations*, which will give rise to a nonzero vector sum, i.e., polarity formation. This is all about a basic mechanism by which growth-induced polarity in molecular crystals can evolve.

Attachment of a next layer on top of the previous one (which, in turn, is considered to act as a rigid substrate) sets up the same type of system that we just have been discussing.

(8) (a) Quintel, A.; Hulliger, J.; Wübbenhorst, M. *J. Phys. Chem. B* **1998**, *102*, 4277. (b) Quintel, A.; Roth, S. W.; Hulliger, J.; Wübbenhorst, M. *Mol. Cryst. Liq. Cryst.* **2000**, *338*, 243.

(9) Rechsteiner, P.; Hulliger, J.; Flörsheimer, M. *Chem. Mater.* **2000**, *11*, 3296.

(10) Hulliger, J. *Chimia* **2001**, *55*, 554.

In general terms, we consider thermalization of an adlayer on top of a substrate layer characterized by a certain density of faulted orientations (disorder). It becomes clear by now that a mechanism of growth taking into account orientational disorder at every attachment layer will give rise to an evolution of polarity just because (i) each layer forms polarity and (ii) orientational faults in the substrate layer are influencing the degree of disorder in the next adlayer (*continuation* or *healing* of defects¹¹).

In the simplest case of coupling, polarity formation can be described by a *Markov-chain* formalism. The probabilities entering a transition matrix may be approached by a Boltzmann description using interaction energies that we define here (see the chapter below).

In real crystals growth may develop in both directions of a substrate. In this case the process of polarity evolution on both sides of symmetry-related growth sectors is equal. Important to notice: The orientations of the resulting vectors of polarization are *opposite* in the "upper" compared to the "lower" sector. Growth-induced polarity is inherently associated with 180° twinning.

It is clear that a mechanism of layer-by-layer thermalization cannot reach the *F* energy minimum corresponding to the *bulk* state of a crystal. Growth-induced effects as described here are producing a *metastable* state of a crystal. However, in many real cases, the energy of activation for a 180° flip of molecules in a particular crystal structure near the surface or in the bulk is far too high for the type of elongated molecules that we have in view here (see Table 1).

Finally we should emphasize that Markov-type polarity formation is not the result of whatever type of a kinetic crystal growth effect, say phenomena produced at conditions of *fast growth*. As outlined above, polarity formation by a layer-by-layer growth mechanism is a growth-induced property that is effected at conditions near to thermodynamic equilibrium, i.e., at a low-driving force for crystal growth.

Throughout the present work, we investigate key properties by means of a *stochastic* analysis. The formalism is kept as general as possible, thus applying to any structural type of molecular crystal built up from dipolar organic molecules, i.e., single-component crystals.

A Markov-mean-field (MMF) model and results using Monte Carlo (MC) simulations are presented. In a precedent paper¹¹ we were discussing cases typical for a low density (up to a few percent) of faulted orientations. For the present work, no restriction with respect to the degree of orientational order/disorder is made.

MMF Model of Polarity Formation in Single-Component Organic Crystals

Further introduction to the Markov-type growth model shall be retrieved from earlier work.^{12,13} In its initial form, we had neglected *lateral* interactions¹³ between neighboring molecules located within an ad-

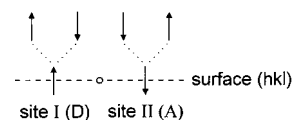


Figure 3. Sites II and I, defined according to Figure 2, where either A or D groups are oriented toward the nutrient. This notation is maintained throughout the text.

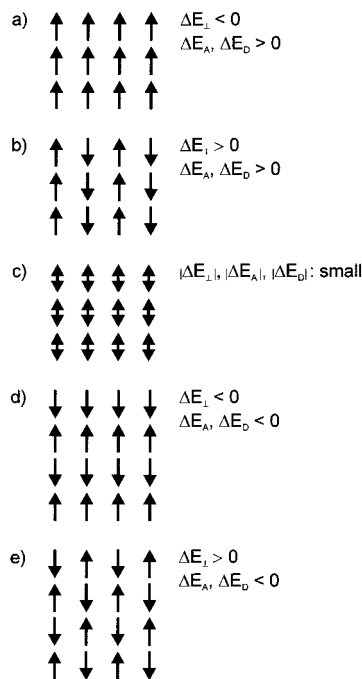


Figure 4. Attempt to classify general packings into basic structures which can arise according to certain couplings, used for Markov model calculations (double arrows represent the case of a 50:50% occupation by dipolar molecules).

layer attached to a substrate layer showing no thermalization (\downarrow vs \uparrow orientation). Here, we present an analysis accounting for both interactions of the adlayer to the substrate and lateral interactions between molecules located within the adlayer.

A preliminary attempt⁶ based on a mean-field approach commonly used to describe solid solutions failed to model precisely the case of predominant *antiparallel* ($\downarrow\cdots\uparrow$) ordering. The present approach is following up ideas put forward in the case of a low density of defects.¹¹ We therefore assume perfect *antiparallel* ordering being perturbed by orientational defects. During the process of attachment to a crystal surface (Figure 2), incoming molecules encounter at least two sites I(D) (D = donor-type fragment) and II(A) (A = acceptor-type fragment attached to an elongated spacer), where the arrow means a vector pointing from D to A; (see Figure 3) at which the attachment probabilities for the \downarrow and \uparrow orientations generally are different.

In view of the symmetry of seed crystals subjected to a mechanism of polarity formation during growth, we consider here the attachment to (*hkl*) faces of a *centric* seed structure (Figure 2a) and to (*hkl*) faces of a *polar*

(11) Hulliger, J.; Alaga-Bogdanovic, M.; Bebie, H. *J. Phys. Chem. B* **2001**, *105*, 8504.

(12) (a) Harris, K. D. M.; Jupp, P. E. *Proc. R. Soc. London A* **1997**, *453*, 333. (b) Harris, K. D. M.; Jupp, P. E. *Chem. Phys. Lett.* **1997**, *274*, 525.

(13) (a) Hulliger, J.; Rogin, P.; Quintel, A.; Rechsteiner, P.; König, O.; Wübbenhorst, M. *Adv. Mater.* **1997**, *9*, 677. (b) König, O.; Bürgi, H.-B.; Armbruster, T.; Hulliger, J.; Weber, T. *J. Am. Chem. Soc.* **1997**, *119*, 10632. (c) Hulliger, J.; Langley, P. J.; König, O.; Roth, S. W.; Quintel, A.; Rechsteiner, P. *Pure Appl. Opt.* **1998**, *7*, 221. (d) Roth, S. W.; Langley, P. J.; Quintel, A.; Wübbenhorst, M.; Rechsteiner, P.; Rogin, P.; König, O.; Hulliger, J. *Adv. Mater.* **1998**, *10*, 1543.

seed structure (Figure 2b). The main part of the theoretical analysis will address polarity formation upon centric seeds. Comments on peculiar phenomena predicted for the growth upon polar faces are given at the end of the chapter dealing with theoretical predictions.

It may also be that we have only one site in a crystal with respect to positions I and II showing a 50:50% occupation by each dipolar orientation. In this case, I(D) and II(A) correspond to either of the two orientations. A further case may arise if layers of altered orientations are formed. Here, arguments given in the Introduction would apply to each of the layers separately. A number of typical layer-type arrangements that we address to describe are shown in Figure 4: In Figure 4a we show a packing for a polar (pyroelectric) symmetry group, whereas in Figure 4b we have the case that we will discuss in detail below. Figure 4c refers to a case where a 50:50% occupation of both dipolar orientations "up" and "down" is present. Finally, with Figure 4d,e we would like to draw attention to systems with an alternating sequence of layers.

Whatever the real packing of molecules may be, any intermolecular coupling providing that $P_{hkl}^I(\uparrow)/P_{hkl}^I(\downarrow) \neq P_{hkl}^{II}(\downarrow)/P_{hkl}^{II}(\uparrow)$ (P = probability for an "up" or "down" orientation to be built into the adlayer; process taking place at a crystal face (hkl); Figures 2 and 3) will give rise to the formation of polarity at each new adlayer as the process of growth proceeds.

We describe here the process of the \downarrow vs \uparrow attachment equilibria at sites I and II by two independent Markov chains accounting each for I or II. This corresponds to the model that was previously applied to channel-type inclusion compounds.¹³

To include the effect of faulted orientations in the nearest neighborhood of a defect, a mean-field correction is introduced. For the calculation of probabilities $P^i(\uparrow) = P_{DA}^I$, $P^i(\downarrow) = P_{DD}^I$, $P^{II}(\downarrow) = P_{AD}^{II}$, and $P^{II}(\uparrow) = P_{AA}^{II}$, we use normalized Boltzmann factors and interaction energies E_{AD} , E_{DD} , E_{AA} , E_{ap} , and E_p (with E_{AD} being the interaction, a synthon,¹⁴ formed between A and D functional groups belonging to molecules of the adlayer and the substrate, respectively, etc., and E_{ap} the lateral interaction for an antiparallel arrangement in the adlayer and E_p that for a parallel arrangement). Mean values for molar fractions X_A^i and X_D^i (index A = acceptor-type molecular fragment oriented toward the nutrient; index D = correspondingly; $i = I$ and II; X_A^I = fraction of \downarrow orientation at site I; X_D^I = fraction of \uparrow orientation at site I, etc.) fulfill normalization conditions: $X_A^i + X_D^i = 1$, $i = I$ and II. In the terminology of faulted orientations, X_A^I and X_D^{II} represent the fractions of faulted orientations at each site I and II (see Figure 3). The 2×2 Markov matrix notations

$$\begin{pmatrix} X_A^I \\ X_D^I \end{pmatrix} = \begin{pmatrix} P_{AD}^I & P_{DD}^I \\ P_{AA}^I & P_{DA}^I \end{pmatrix}^q \begin{pmatrix} 0 \\ 1 \end{pmatrix} \quad (1)$$

$$\begin{pmatrix} X_A^{II} \\ X_D^{II} \end{pmatrix} = \begin{pmatrix} P_{AD}^{II} & P_{DD}^{II} \\ P_{AA}^{II} & P_{DA}^{II} \end{pmatrix}^q \begin{pmatrix} 1 \\ 0 \end{pmatrix} \quad (2)$$

reduce to ($q = 1, 2, \dots, \infty$, the number of layers being

attached)

$$X_A^I = \frac{P_{DD}^I}{P_{DD}^I + P_{AA}^I} \quad (3)$$

$$X_D^{II} = \frac{P_{AA}^{II}}{P_{AA}^{II} + P_{DD}^{II}} \quad (4)$$

Probabilities are given by

$$P_{jj}^i = \frac{1}{1 + f_j^i}, \quad i = I, II, j = A, D \quad (5)$$

For a definition of the f_j^i functions, see below. Basic equations describing corresponding fractions X of faulted orientations at sites I and II result from eqs 3–5:

$$X_A^I = \frac{1 + f_A^I}{2 + f_A^I + f_D^I} \quad (6)$$

$$X_D^{II} = \frac{1 + f_D^{II}}{2 + f_D^{II} + f_A^{II}} \quad (7)$$

The net fraction of dipoles with orientation \downarrow (presenting acceptor-type fragments A to the crystal–nutrient interface) is defined by

$$X_{\text{net}}(\downarrow) \equiv X_{\text{net}} \equiv X_A^I - X_D^{II} \quad (8)$$

(for the case of the growth on a centric seed, see also ref 11).

Corresponding f_j^i functions are

$$f_D^I = \exp\{[\Delta E_D + z_{\perp} \Delta E_{\perp}(1 - 2X_D^{II})]/RT\} \quad (9)$$

$$f_A^I = \exp\{[\Delta E_A - z_{\perp} \Delta E_{\perp}(1 - 2X_D^{II})]/RT\} \quad (10)$$

$$f_D^{II} = \exp\{[\Delta E_D - z_{\perp} \Delta E_{\perp}(1 - 2X_A^I)]/RT\} \quad (11)$$

$$f_A^{II} = \exp\{[\Delta E_A + z_{\perp} \Delta E_{\perp}(1 - 2X_A^I)]/RT\} \quad (12)$$

where $\Delta E_D = E_{DD} - E_{AD}$, $\Delta E_A = E_{AA} - E_{AD}$, $\Delta E_{\perp} = E_p - E_{ap}$, and z_{\perp} = number of nearest neighbors within the adlayer (\perp denotes the lateral direction).

The present set of coupled nonlinear equations (eqs 6, 7, and 9–12) was solved numerically. For a comparison, MC simulations were performed. For MC runs we have assumed an adlayer (being thermalized) on top of a substrate layer (not being thermalized). Details of the MC procedure are discussed elsewhere.¹¹

Predictions of the Stochastic Model

In the frame of a two-dimensional Markov-type description, we implicitly make the assumption of an average value in calculating the macroscopic vector sum of individual dipoles: At first there is averaging at each adlayer. Second we are interested in the limit of X_{net} after a large number q of added layers ($q = 10\text{--}10^6$), say in the growth to macroscopic size. In real crystals it may happen that around the seed polarization develops because of either a steep or a very flat gradient,

(14) Desiraju, G. R. *Angew. Chem., Int. Ed. Engl.* **1996**, *34*, 2328.

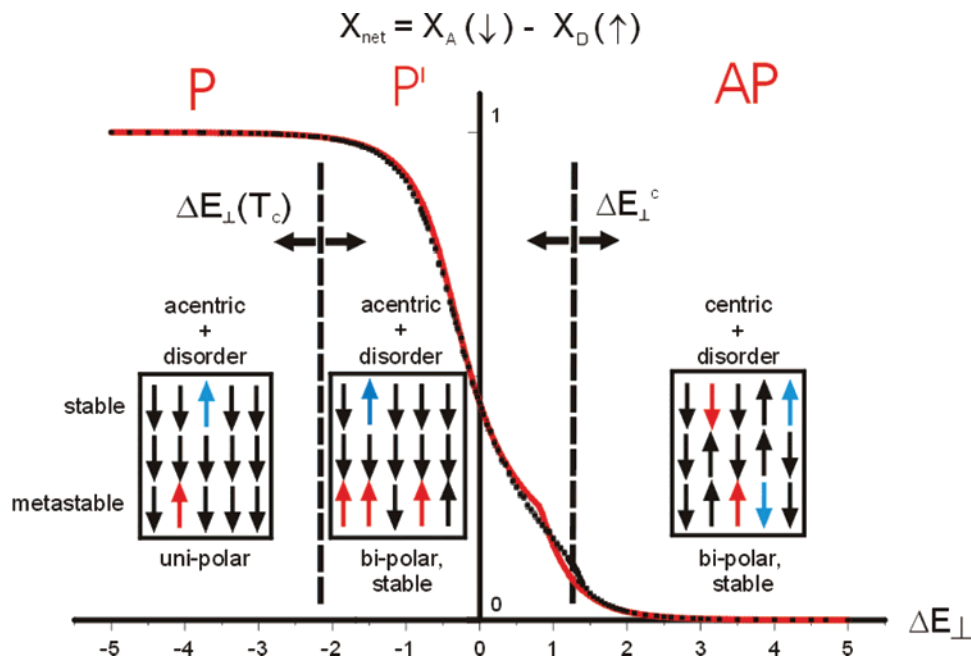


Figure 5. Basic illustration to show the influence of lateral coupling ΔE_{\perp} on polarity formation as obtained by the growth model. P: polar (P) structure type a in Figure 3 at site II (A). P': region where many orientational defects occur. AP: structure type b in Figure 4. For calculations we used the following: (i) red curve, eqs 6–12; (ii) single points, MC simulation. $\Delta E_A = 5$, $\Delta E_D = 2$, $T = 300$ K, $z_{\perp} = 4$. ΔE_{\perp}^c is indicating a phase transition. Below $\Delta E_{\perp}(T_c)$ the probability for 180° switching of most of the dipoles at sites I(D) is very low and may not happen because in real crystals we have a finite number of attached layers.

reaching therefore a constant X_{net} value after a few nanometers up to a few microns, depending on the intermolecular coupling constants ΔE_A , ΔE_D , and ΔE_{\perp} .

Put forward as general as possible, nonfaulted (ideal) configurations as shown in Figure 4 may result, because of limiting values for ΔE_A , ΔE_D , and ΔE_{\perp} : In Figure 4a, a negative ΔE_{\perp} and positive ΔE_A and ΔE_D stabilize a polar configuration. In Figure 4b, ΔE_A , ΔE_D , and a positive ΔE_{\perp} give rise to a centric state. In Figure 4c, small absolute values of all coupling parameters allow for packing, which is similar as formed by symmetrical molecules showing no dipole moment (indicated here by double arrows). In Figure 4d,e, negative ΔE_A and ΔE_D values and ΔE_{\perp} (negative or positive) favor head-to-head and tail-to-tail bilayers, respectively. In the strong coupling limit of ΔE_{\perp} (Figure 4a–e) and grown at room temperature, all of these “structures” will show no significant orientational disorder. However, there are ranges for ΔE_A , ΔE_D , and ΔE_{\perp} where each of them can exceed a significant reduction (Figure 4a) or an increase (Figure 4b–e) of X_{net} .

To give an illustration, let us discuss here the change from the antiparallel (Figure 4b) to the parallel (Figure 4a) state: In Figure 5, X_{net} was calculated using the MMF (red curve) model and MC simulations (points). For the purpose of our discussion, the agreement of both approaches is sufficient in order to use only analytical calculations to gain an idea about the temperature dependence (Figure 7). At given values for ΔE_A , ΔE_D , z_{\perp} , and T , X_{net} is shown as a function of only the lateral coupling:

For largely negative ΔE_{\perp} values, we obtain the structure type of Figure 4a. On the contrary, at large positive ΔE_{\perp} , the one in Figure 4b is formed. In between, there is a window for ΔE_{\perp} , for which considerable disorder is predicted. Although we have limited ΔE_A and $\Delta E_D > 0$ to a certain range (ΔE_A and $\Delta E_D < 25$ kJ/mol,

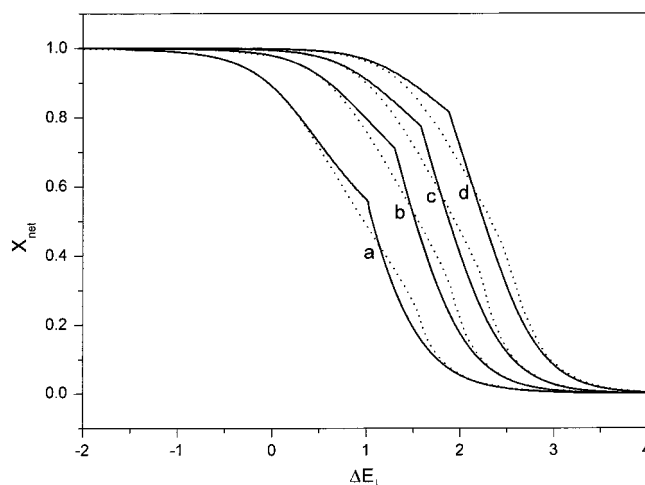


Figure 6. Similar to Figure 5 we show here the influence of parameters ΔE_A and ΔE_D on polarity formation. Solid lines: (a) $\Delta E_A = 10$, $\Delta E_D = 2$; (b) 15, 3; (c) 20, 5; (d) 25, 7; correspondingly. Points: MC simulation. For chemically realistic values of ΔE_A and ΔE_D , significant deviations from structure types a and b in Figure 4 are obtained between -2 and 4 kJ/mol for ΔE_{\perp} ($T = 300$ K, $z_{\perp} = 4$). Calculated by use of eqs 6–12.

$z_{\perp} = 4$), the curves given in Figure 6 reveal a generality which may apply to all organic crystals that we have in view here: Within the range of about -2 kJ/mol $\leq \Delta E_{\perp} \leq 3$ –4 kJ/mol ($z_{\perp} = 4$, $T = 300$ K), crystals can develop a level of orientational disorder which for $\Delta E_{\perp} < 0$ is leading to a reduction of the polarity, whereas for $\Delta E_{\perp} > 0$, all near to centric structures can become effectively acentric. In between perfect structures (Figure 4a,b), there is a ΔE_{\perp}^c value where through a phase transition¹⁵ a quasi-paraelectric phase transforms into a faulted

(15) Bebie, H.; Hulliger, J.; Eugster, S.; Alaga-Bogdanovic, M. *Phys. Rev. E* **2001**, submitted for publication.

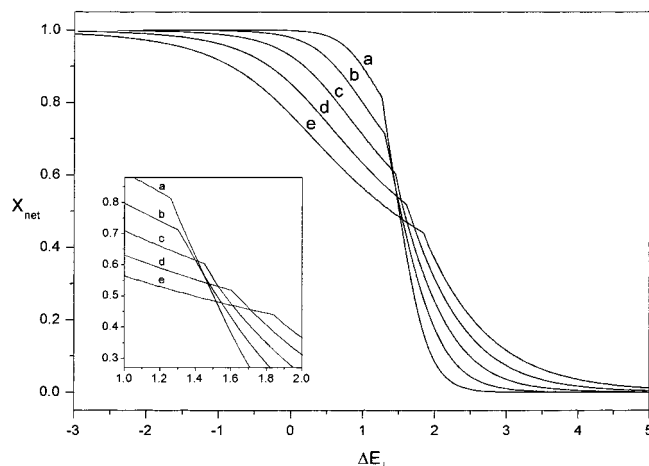


Figure 7. Variation of ΔE_{\perp}^c as a function of temperature, calculated from eqs 6–12 and $\Delta E_A = 15$, $\Delta E_D = 3$, $z_{\perp} = 4$, for (a) $T = 200$ K, (b) $T = 300$ K, (c) $T = 400$ K, (d) $T = 500$ K, and (e) $T = 600$ K.

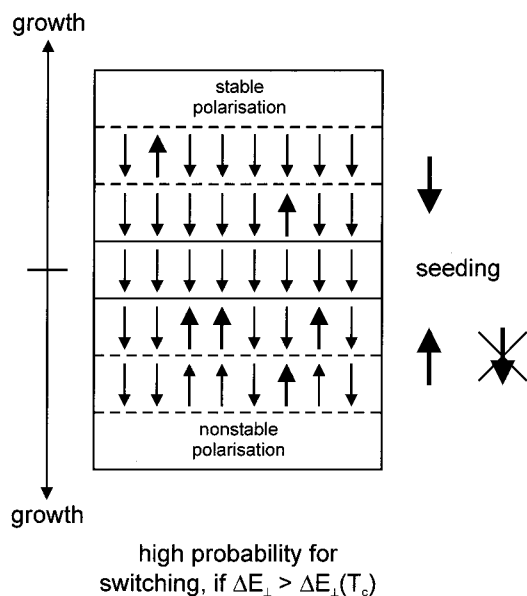


Figure 8. Diagram illustrating the switching process. For a given sign of ΔE_{\perp} , growth at II(A) sites of a polar crystal can occur in stable mode, whereas at the I(D) sites, there is an instability against 180° switching of most of the arrows. Switching will convert a single crystalline seed into a macroscopically bipolar object.

antiparallel packing of dipoles. As a result of the MMF model, the phase transition is indicated by a kink. Because experimentally we cannot vary ΔE_{\perp} for a given crystal, it is interesting to investigate the temperature shift of the energy where this transition might occur. According to Figure 7, a change of the growth temperature may give rise to polymorphism with respect to orientational order ($\Delta E_{\perp}(T)$ is assumed to be constant for a variable T).

There is another peculiarity of the system: Typically, below $\Delta E_{\perp}(T_c)$, the value for Onsager's exact solution of the Ising two-dimensional model in zero field,¹⁶ growth along *one* direction of a polar axis may undergo a 180° flip of most of the dipoles (Figure 8), just because site I(D) is not stable against such a flipping process

(for ΔE_A and $\Delta E_D > 0$ and $\Delta E_A > \Delta E_D$). Given conditions as noted above, growth at site II(A) of a structure type shown in Figure 4a will develop in a stable manner. Alternatively, in case I (Figure 4a) we may end up in a metastable state, just because switching at I(D) sites did not take place after a finite number of layers q attached to this side of a growing crystal. In Figure 8 we describe a situation where at the lower side (I) of a growing crystal the Markov mechanism has effected a 180° flip of some of the dipoles. When growth proceeds at this side (I), most of the dipoles previously pointing "downward" will be turned in arrows oriented "upward".

Organic Materials Providing Evidence for Growth-Induced Polarity

Organic solid solutions¹⁷ and channel-type inclusion compounds¹⁸ were the first materials to show growth-induced polarity. Application of SPEM⁸ and PS-SHM⁹ confirmed the bipolar state of growth for inclusion compounds of perhydrotriphenylene⁷ and a dumbbell-shaped host molecule.¹⁹ In view of a large number of crystal structures obtained by crystallization of *single-component* dipolar compounds, including that the majority of these structures are found to be *centric*,²⁰ we stay just at the beginning of a reinvestigation focusing on minor or pronounced effects of polarity in molecular crystals.

At first we may set up criteria for searching typical examples. Because of the parametrization given by the present model, we shall distinguish crystal structures featuring (i) *strong* functional group interactions (synthons) from those (ii) that do not show strong intermolecular binding motifs. Packing types a, b, d, and e (Figure 4) are obtained by MC simulations if synthon interactions are present. Type c will show up in the case of weak interactions. Examples for both classes i and ii are listed in Table 1. Second harmonic generation (SHG) effects were observed for all materials, although centric structures were assigned by X-ray diffraction. Because of polymorphic forms (minority phase in polycrystalline samples), SHG was measured for a number of small single crystals ($d < 50\text{--}100 \mu\text{m}$), prepared according to the description in original crystallographic publications listed in Table 1. These results account for the existence of a significant level of orientational disorder in crystal structures reported to be centric.

From the present examples, we conclude that the Cl- π -NO₂ compound falls into class ii, whereas HC \equiv C- π -CN, HC \equiv C- π -NO₂, Br- π -CN, and I- π -CN compounds can give rise to a packing driven by synthons (i). In general, materials expected to show pronounced growth-induced polarity effects may be those where (a) the spacer (π) is fairly long and rigid, (b) synthon interactions are present, and (c) the van der Waals surfaces of A and D functional groups are similar.

Experimental Details

Preparation of Crystals. (i) *Temperature Lowering.* A total of 5–10 mg of the compounds **1** and **3–5** was dissolved

(17) Vaida, M.; Shimon, L. J.; Weisinger-Lewin, Y.; Frolow, F.; Lahav, M.; Leiserowitz, L.; McMullin, R. K. *Science* **1988**, *241*, 1475.

(18) (a) Eaton, D. F.; Anderson, A. G.; Tam, W.; Wang, Y. *J. Am. Chem. Soc.* **1987**, *109*, 1886. (b) Tam, W.; Eaton, D. F.; Calabrese, J.; Williams, I.; Wang, Y.; Anderson, A. G. *Chem. Mater.* **1989**, *1*, 128.

(19) Müller, T.; Hulliger, J.; Seichter, W.; Weber, E.; Weber, T.; Wübberhorst, M. *Chem. Eur. J.* **2000**, *6*, 54.

(16) Onsager, L. *Phys. Rev.* **1944**, *65*, 117.

in 2 mL of hot ethanol. After slow cooling to room temperature, single crystals were collected.

(ii) *Sublimation*. A total of 5–10 mg of the compounds **2** and **8** was sublimed in an evacuated and sealed glass tube at the given conditions (Table 1). After crystallization, the purity of all compounds was tested by gas chromatography.

SHG Measurements. For SHG experiments a Continuum SLI-10 nanosecond pulsed Nd:YAG laser ($\lambda_0 = 1064$ nm) was used. Single crystals of each compound were crashed between two glass slides for a qualitative measurement of frequency doubling at a peak power of 30 MW/cm² (in comparison to a sample of urea, prepared in the same way).

X-ray Crystallography of 4-Chloro-4'-nitrostilbene: C₁₄H₁₀ClNO₂; $M = 259.68$; space group $P2_1/c$; $a = 3.8364(10)$ Å, $b = 12.916(2)$ Å, $c = 12.221(3)$ Å, $\alpha = 90^\circ$, $\beta = 93.91(3)^\circ$, $\gamma = 90^\circ$, $V = 604.2(2)$ Å³, $Z = 2$, $D_c = 1.427$ g/cm³, $\mu = 0.308$ mm⁻¹. Intensity data were collected at 153 K on a Stoe Image plate diffraction system using Mo K α graphite-monochromated radiation. Image plate distance 70 mm, ϕ oscillation scans 0–200°, step $\Delta\phi = 1.5^\circ$, 2θ range 3.27–52.1°, and $d_{\max} - d_{\min} = 12.45 - 0.81$ Å. The structure was solved by direct methods using the program SHELXS-97. The refinement and all further calculations were carried out using SHELXL-97. The H atoms were included in calculated positions and treated as riding atoms using SHELXL default parameters. The non-H atoms were refined anisotropically; using weighted full-matrix least squares on F^2 . Final $R = 0.0727$ (observed), 0.1116 (all); $wR_2 = 0.1628$ (observed), 0.1783 (all).

Conclusions

For the first time, an analytical model is presented which describes growth-induced spontaneous polarity formation in single-component organic crystals ($X_{\text{net}} \gg 0.01$). As demonstrated numerically, there can be attributed a range of lateral coupling (-2 kJ/mol $\leq \Delta E_{\perp} \leq 3-4$ kJ/mol, $z_{\perp} = 4$, $T = 300$ K) where, nearly independent of realistic values for functional group interactions (A and D; Figure 6), significant polarity is evolving when lowering ΔE_{\perp} from the side of largely positive values (Figure 5). In the general case, a crystalline single-component material may fall into one of the real structures classified by AP, P', or P (Figure 5).

(i) AP: At $\Delta E_{\perp} > \Delta E_{\perp}^c$, the structure will show some orientational disorder, which is decreasing as ΔE_{\perp} gets largely positive. Polarity that is formed at faces (hkl) and ($\bar{h}\bar{k}\bar{l}$) is numerically equal, but resultant vectors of polarization (vector sum; see Introduction) show an opposite orientation.

(ii) P: At $\Delta E_{\perp} \leq \Delta E_{\perp}^c$ (T_c), the structure is polar, although showing some orientational disorder, which is reducing the total polarization that the system can build up. As compared to AP, nonsymmetry-related faces (hkl) and ($\bar{h}\bar{k}\bar{l}$) show a completely different behavior: Given the sign of the difference $\Delta E_f = \Delta E_A - \Delta E_D$, one direction of growth is developing some defects (stable),

(20) According to the 5.2 update of the Cambridge Crystallographic Database, 76% of the entries are centrosymmetric.

whereas the opposite one becomes metastable against a 180° flipping of most of the dipoles (Figure 8). As a result of the basic property of the Markov model, the process of flipping can occur at a high or even at a low density of orientational defects. Here, we predict a fundamentally new growth-induced property of polar crystals: There is some probability for a growth-induced 180° twinning which differs from geometrical twinning known in crystallography. Markov-type twinning is a *continuous process*, which develops as growth proceeds.

(iii) P': There is a window between borders that we have drawn into Figure 5 where nominally polar/centric structures are exceeding a significant decrease/increase of polarity, respectively, because of the effect of strong 180° orientational disorder. The case of $\Delta E_{\perp} = 0$ is particularly well documented by channel-type inclusion compounds. Both the left and right borderlines in Figure 5 can be shifted with temperature (see Figure 7).

In view of *crystal engineering* of polar materials, we conclude the following: (i) Medium to strong functional group interactions are needed; otherwise, the structure may fall into a case where a structure refinement puts the center of symmetry onto the molecular site (fractional occupation by "up" and "down" orientations), case c in Figure 4. (ii) A value of $|\Delta E_f| = |\Delta E_A - \Delta E_D| \geq 3$ ($T = 300$ K, $z_{\perp} = 4$) is in favor of polarity. (iii) Any value of $\Delta E_{\perp} > 0$ is lowering the polarity as compared to the situation at $\Delta E_{\perp} = 0$.

As a result of extended numerical analyses, we find that the synthetic playground for tuning *lateral interactions* is rather limited: Above a $\Delta E_{\perp} \geq 3$ kJ/mol and even at large ΔE_f values, a strong drop of polarity is predicted. Being aware of developing here nothing but a *growth* model, we anticipate that structures showing a ΔE_{\perp} larger than 3 kJ/mol may crystallize in a centric point group (AP case), essentially independent of a realistic strength of typical synthon interactions.

Synthetic work aiming to provide examples showing new phenomena that we predict here is in progress.

Acknowledgment. This work was supported by the Swiss NRP "Supramolecular Functional Materials" Project No. 4047-057476/1.

CM010405Y

(21) Thalladi, V. R.; Goud, B. S.; Hoy, V. J.; Allen, F. H.; Howard, J. A. K.; Desiraju, G. R. *Chem. Commun.* **1996**, 401.

(22) Kronebusch, P.; Gleason, W. B.; Britton, D. *Cryst. Struct. Commun.* **1976**, 5, 17.

(23) Gleason, W. B.; Britton, D. *Acta Crystallogr., Sect. C* **1991**, 47, 2127.

(24) Langley, P. J.; Hulliger, J.; Thaimattam, R.; Desiraju, G. R. *New J. Chem.* **1998**, 22, 1307.

(25) Graham, E. M.; Miskowski, V. M.; Perry, J. W.; Coulter, D. R.; Stiegman, A. E.; Schaefer, W. P.; Marsh, R. E. *J. Am. Chem. Soc.* **1989**, 111, 8771.

(26) Wang, Y.; Tam, W.; Stevenson, S. H.; Clement, R. A.; Calabrese, J. *Chem. Phys. Lett.* **1988**, 148, 136.